Article

SOURCE DATA | TRANSPARENT PROCESS

THE EMBO JOURNAL

Mfn2 deficiency links age-related sarcopenia and impaired autophagy to activation of an adaptive mitophagy pathway

David Sebastián[1,2,3], Eleonora Sorianello[1,2,3], Jessica Segalés[1,2,3], Andrea Irazoki[1], Vanessa Ruiz-Bonilla[4], David Sala[1,2,3,†], Evarist Planet[1], Antoni Berenguer-Llergo[1], Juan Pablo Muñoz[1,2,3], Manuela Sánchez-Feutrie[1,2,3], Natàlia Plana[1,2,3], María Isabel Hernández-Álvarez[1,2,3], Antonio L Serrano[4], Manuel Palacín[1,2,5] & Antonio Zorzano[1,2,3,*]

Abstract

Mitochondrial dysfunction and accumulation of damaged mitochondria are considered major contributors to aging. However, the molecular mechanisms responsible for these mitochondrial alterations remain unknown. Here, we demonstrate that mitofusin 2 (Mfn2) plays a key role in the control of muscle mitochondrial damage. We show that aging is characterized by a progressive reduction in Mfn2 in mouse skeletal muscle and that skeletal muscle Mfn2 ablation in mice generates a gene signature linked to aging. Furthermore, analysis of muscle Mfn2-deficient mice revealed that aging-induced Mfn2 decrease underlies the age-related alterations in metabolic homeostasis and sarcopenia. Mfn2 deficiency reduced autophagy and impaired mitochondrial quality, which contributed to an exacerbated age-related mitochondrial dysfunction. Interestingly, aging-induced Mfn2 deficiency triggers a ROS-dependent adaptive signaling pathway through induction of HIF1α transcription factor and BNIP3. This pathway compensates for the loss of mitochondrial autophagy and minimizes mitochondrial damage. Our findings reveal that Mfn2 repression in muscle during aging is a determinant for the inhibition of mitophagy and accumulation of damaged mitochondria and triggers the induction of a mitochondrial quality control pathway.

Keywords aging; autophagy; mitochondria; mitophagy; sarcopenia
Subject Categories Ageing; Autophagy & Cell Death; Membrane & Intracellular Transport
DOI 10.15252/embj.201593084 | Received 30 September 2015 | Revised 25 May 2016 | Accepted 27 May 2016

Introduction

Aging is a process characterized by a progressive accumulation of damage that leads to tissue dysfunction and failure. Skeletal muscle is one of the tissues most affected by aging. During aging, there is a gradual loss of muscle mass and function (sarcopenia), which are associated with frailty and a reduction in quality of life in the elderly (Cesari *et al*, 2014). In addition, skeletal muscle alterations play a central role in aging-associated metabolic dysregulation (Dela & Kjaer, 2006). Therefore, understanding the molecular mechanisms causing aging-induced skeletal muscle alterations is of great importance for healthy aging (de Cabo *et al*, 2014).

A hallmark of aging is the presence of a decline in mitochondrial function in skeletal muscle associated with accumulation of mitochondrial damage, abundant morphological alterations in mitochondria (e.g., rounded and giant mitochondria), reduced mitochondrial respiration, and increased oxidative stress (Shigenaga *et al*, 1994; Preston *et al*, 2008; Artal-Sanz & Tavernarakis, 2009; Bratic & Larsson, 2013). Recent data indicate that aging is characterized by impaired mitophagy in C. *elegans*, which may explain the accumulation of damaged mitochondria (Palikaras *et al*, 2015). However, there is still debate about whether mitochondrial deficiency could be driving some of the age-related alterations or on the contrary, age-associated mitochondrial dysfunction might be secondary to aging itself (Bratic & Larsson, 2013).

Mitochondrial dynamics is a crucial process not only for mitochondrial morphology but also in the control of mitochondrial function, response to apoptotic stimuli, and mitochondrial quality control (Twig *et al*, 2008; Liesa *et al*, 2009). Mitochondrial dynamics is controlled by fusion and fission proteins. Mitofusin 1 and 2 (Mfn1/2) proteins are involved in the outer mitochondrial membrane fusion, whereas optic atrophy 1 (OPA1) protein is

1 Institute for Research in Biomedicine (IRB Barcelona), The Barcelona Institute of Science and Technology, Barcelona, Spain
2 Departament de Bioquímica i Biomedicina Molecular, Facultat de Biologia, Universitat de Barcelona, Barcelona, Spain
3 Centro de Investigación Biomédica en Red de Diabetes y Enfermedades Metabólicas Asociadas (CIBERDEM), Instituto de Salud Carlos III, Madrid, Spain
4 Cell Biology Group, Department of Experimental and Health Sciences, Pompeu Fabra University (UPF), CIBER on Neurodegenerative diseases (CIBERNED), Barcelona, Spain
5 Centro de Investigación Biomédica en Red de Enfermedades Raras (CIBERER), Instituto de Salud Carlos III, Madrid, Spain
*Corresponding author. Tel: +34 93 403 7197; E-mail: antonio.zorzano@irbbarcelona.org
†Present address: Development Aging and Regeneration Program (DARe), Sanford Burnham Prebys Medical Institute, La Jolla, CA, USA

© 2016 The Authors

involved in fusion of the inner mitochondrial membrane. Fission of mitochondria is controlled by Fis1, Drp1, and Mff proteins. A correct balance between fusion and fission is essential for mitochondrial function and cellular homeostasis (Liesa & Shirihai, 2013).

Besides its role in mitochondrial fusion, Mfn2 has been described to be involved in the regulation of cell proliferation, oxidative metabolism, autophagy, mitophagy, mitochondrial antiviral signaling, and unfolded protein response (Bach *et al*, 2003; Chen *et al*, 2004; Yasukawa *et al*, 2009; Hailey *et al*, 2010; Ngoh *et al*, 2012; Zhao *et al*, 2012; Chen & Dorn, 2013; Munoz *et al*, 2013). Recently, we have elucidated the role of Mfn2 in skeletal muscle *in vivo*. Deficiency of Mfn2 in skeletal muscle leads to reduced mitochondrial respiration and increased oxidative stress leading to inhibition of insulin signaling. As a result, high-fat-fed Mfn2-deficient mice show glucose intolerance and greater insulin resistance, which highlights the importance of Mfn2 in the maintenance of normal muscle metabolism (Sebastian *et al*, 2012).

Here, we analyzed the role of Mfn2 during aging. We show that Mfn2 protein expression decreases during aging in skeletal muscle and deficiency of Mfn2 in young mice aggravates the age-associated whole-body metabolic alterations and sarcopenia, mainly as a result of impaired autophagy and mitochondrial quality. Furthermore, aging and reduction in Mfn2 trigger an adaptive signaling pathway involving HIF1α in order to minimize the accumulation of damaged mitochondria. Overall, the data presented here describe a new role for Mfn2 connecting mitochondrial function and quality to the maintenance of metabolism and muscle fitness during aging.

Results

Mfn2 expression in skeletal muscle decreases during aging and generates a gene signature characteristic of aged muscle

It has not been evaluated in mammals whether mitochondrial dynamics has an impact on aging. Based on the functional relevance of mitochondrial fusion and fission factors, we decided to analyze whether the mitochondrial fusion protein mitofusin 2 (Mfn2) plays a role in aging. We show that Mfn2 protein expression is markedly reduced in skeletal muscles in old mice (Figs 1A and EV1A), to a lesser extent in heart and no changes were detectable in liver (Fig EV1B). Mfn2 downregulation occurred in the absence of changes in the expression of other mitochondrial proteins such as Porin or ATP5a (Fig 1A). Moreover, analysis of Mfn2 expression in young adult (6-month-old), middle aged (12-month-old), and old (22-month-old) mice revealed that the decrease of Mfn2 protein expression was progressive during aging (Fig EV1C). Reduction in Mfn2 was not a consequence of reduced gene expression (Fig EV1D) or lower availability of Mfn2 mRNA for translation, as indicated by the lack of changes of Mfn2 mRNA levels in polysomal fractions, containing actively translated mRNAs bound to ribosomes (Fig EV1E). These results suggest that reduced Mfn2 expression in aged muscle may be a consequence of changes in protein turnover. In addition to Mfn2, the expression of other mitochondrial dynamics proteins, such as Mfn1, OPA1, and Fis1 but not Drp1, was reduced during aging in skeletal muscle (Fig EV1F).

To gain insight into the consequences of Mfn2 repression in muscle during aging, and the identification of the mechanisms involved, we used Mef2C-Cre$^{+/-}$Mfn2$^{LoxP/LoxP}$ mice (Mfn2KO mice) as reported previously (Sebastian *et al*, 2012). Mfn2KO mice showed an 80% reduction in Mfn2 expression in muscle and heart, and a 50% reduction in other tissues such as WAT, kidney, or liver (Sebastian *et al*, 2012). We performed transcriptomic analysis in muscle from 6-month-old control and Mfn2KO mice and 22-month-old control and Mfn2KO mice. Deficiency of Mfn2 in skeletal muscle caused a deregulation of 186 genes in young mice and of 53 genes in old mice (Fig 1B). Aging caused a change in expression of 2,550 genes in control mice (Fig 1C). Interestingly, 62% of genes deregulated in Mfn2KO young mice were also altered during aging in control mice (Fig 1B and C, Table EV1). Moreover, these genes were further deregulated in Mfn2KO old mice compared with control old mice (Fig 1C). GSEA analysis of transcriptomic data further revealed that genes deregulated by Mfn2 deficiency were significantly enriched during normal aging in control mice (Fig 1D). These alterations occurred in the absence of changes in the expression of other mitochondrial dynamics proteins in Mfn2KO mice (Fig EV1F). Analysis of life span revealed no changes in Mfn2KO mice compared to control mice (Fig EV1G). Therefore, all these results indicate that Mfn2 decreases with aging in mouse skeletal muscle, which participates in the generation of an aging gene signature.

Mfn2 deficiency in skeletal muscle enhances age-induced mitochondrial dysfunction

Mfn2 controls mitochondrial respiration (Bach *et al*, 2003; Sebastian *et al*, 2012; Segales *et al*, 2013). Therefore, we analyzed mitochondrial oxygen consumption in isolated muscle fibers from young and old control and Mfn2KO mice. Mitochondrial respiration was reduced during aging in control mice and further decreased in old Mfn2KO mice (Fig 2A). These alterations were restricted to skeletal muscle, and other tissues such as liver, heart, and WAT did not show any changes in mitochondrial respiration in Mfn2KO mice (Appendix Figs S1A and S2B and C). Alterations in muscle oxygen consumption were independent of major changes in protein expression of subunits of respiratory electron transport chain (Appendix Fig S1D), mitochondrial mass (Fig 2B), and ATP content in skeletal muscle (Appendix Fig S1E). Glucose oxidation in soleus muscles was also decreased during aging or in Mfn2KO mice (Appendix Fig S1F). NADH-TR and SDH staining were decreased in young Mfn2KO mice and during aging in control mice, and further reduced in old Mfn2KO mice, confirming a decreased oxidative capacity during aging and Mfn2-deficiency conditions (Fig 2C and D). Mfn2 deficiency was also characterized by higher levels of hydrogen peroxide and enhanced protein carbonylation indicating an enhanced oxidative stress (Fig 2E and F). Activity of antioxidant enzymes was modified by aging, but no changes were detected between genotypes, except for glutathione peroxidase, which is increased in young Mfn2KO mice (Appendix Fig S1G–J). Mfn2 reduction was not associated with an increase in mtDNA mutations as evidenced by the lack of changes in the number of COX negative/SDH-positive fibers (Appendix Fig S1K). Ultrastructural morphometric analysis of muscle sections revealed the presence of abnormalities in mitochondria from aged mice such as increased

 © 2016 The Authors

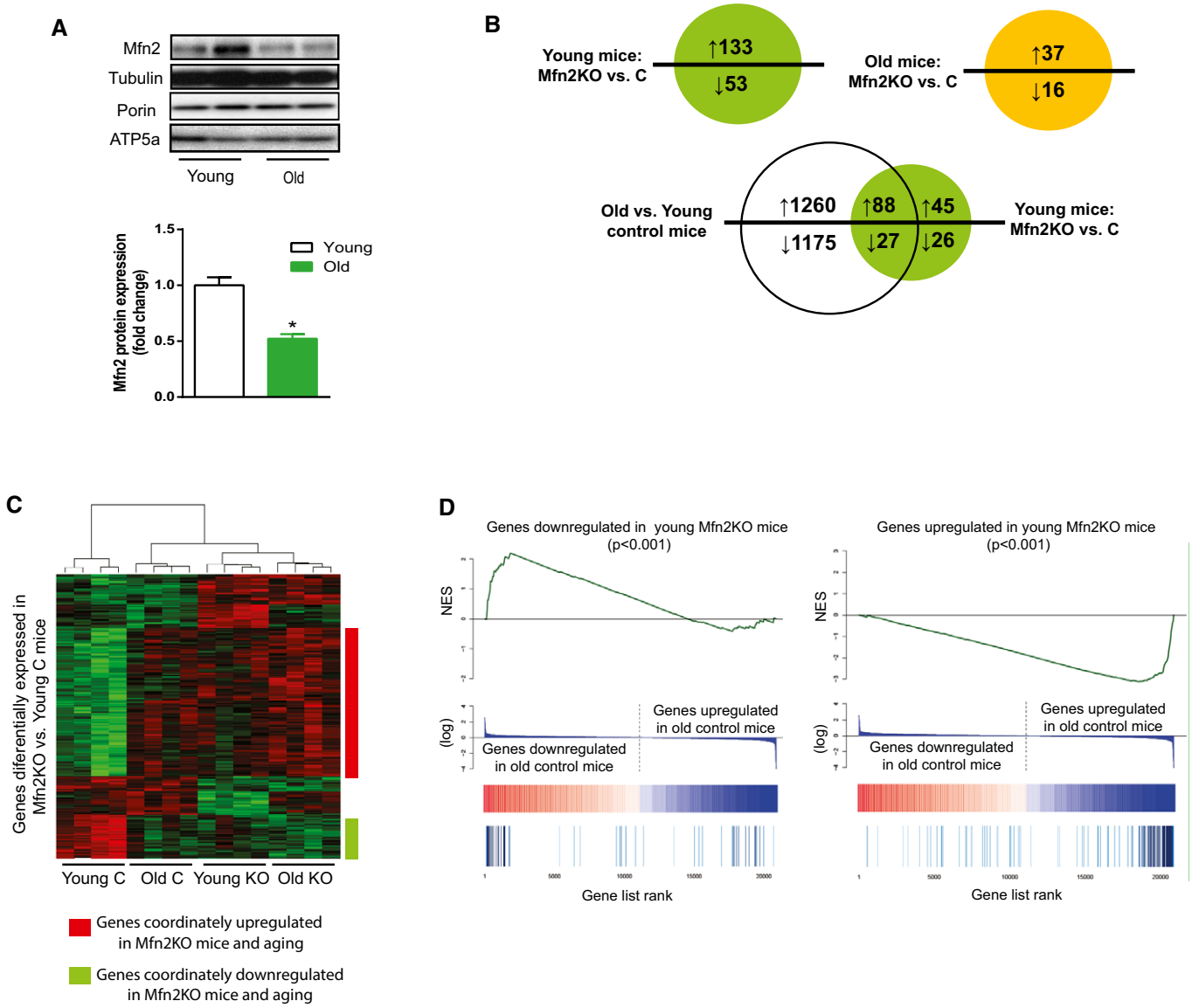

Figure 1. Mfn2 expression decreases during aging in skeletal muscle and generates a gene signature common to aging.

A Mfn2 protein expression was measured in gastrocnemius muscle from young (6-month-old) and old (22-month-old) mice (n = 11–13 mice per group, *P < 0.05). Data were normalized by tubulin and expressed as relative values of young mice.

B Venn diagram depicting genes differentially expressed in Mfn2-deficient muscle and old muscle compared with muscle from young or old control mice.

C Heatmap of genes differentially expressed in Mfn2-deficient muscle.

D GSEA of genes down- and upregulated in Mfn2-deficient muscle in relation to aging in control mice.

Data information: Data represent mean ± SEM and were normalized by tubulin and expressed as relative values of young mice; analyzed by Student's t-test.
Source data are available online for this figure.

mitochondrial area and decreased mitochondrial density (Fig 2G and Appendix Fig S1L). These alterations were more extreme in Mfn2KO old mice (Fig 2G and Appendix Fig S1L). Moreover, Mfn2KO old mice showed a greater abundance of aberrant mitochondria, swollen mitochondria, or organelles with disrupted cristae (Fig 2H). In all, our data indicate that Mfn2 deficiency in skeletal muscle causes the development of age-related alterations in mitochondrial function and are coherent with the view that Mfn2 repression that occurs with aging plays a role in the development of mitochondrial dysfunction in this condition.

Decrease of Mfn2 during aging is a contributing factor for age-related metabolic disorders

Skeletal muscle plays an important role in the maintenance of metabolic homeostasis *in vivo* (Rolfe & Brown, 1997). On the basis of the impact of Mfn2 deficiency on mitochondrial function and oxidative capacity in skeletal muscle, we tested whether these alterations could have a role in the metabolic alterations that are common to aging, such as glucose intolerance, insulin resistance, and lower energy expenditure (Niccoli & Partridge, 2012). Body weight was

© 2016 The Authors

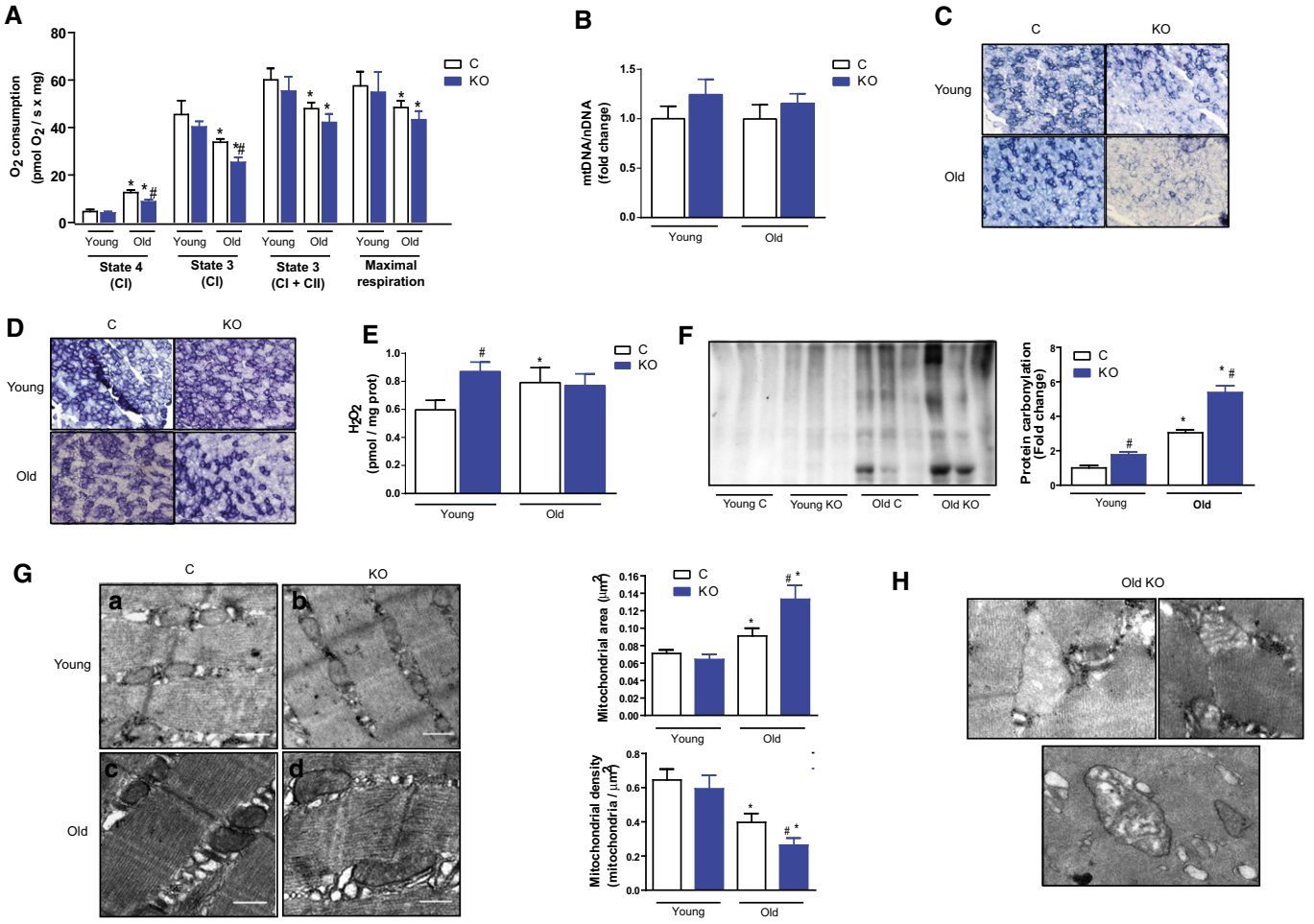

Figure 2. Mfn2-deficient skeletal muscle shows an enhanced age-induced mitochondrial dysfunction.

A Oxygen consumption was analyzed in permeabilized muscle fibers from tibialis muscle from young and old control and Mfn2KO mice (n = 6 mice per group).

B Mitochondrial mass was evaluated by mtDNA copy number in gastrocnemius muscle (n = 6 per group). Data were expressed as a fold change compared to young control mice.

C, D Representative images of NADH-TR staining (C) and SDH staining (D) in muscle sections from young and old control and Mfn2KO mice (n = 3 mice per group).

E Levels of H_2O_2 measured in gastrocnemius muscle from young and old control and Mfn2KO mice (n = 6 mice per group).

F Protein carbonylation was measured in gastrocnemius muscle from young and old control and Mfn2KO mice (n = 6 mice per group). Data were expressed as a fold change compared to young control mice.

G Representative TEM images of longitudinal sections of quadriceps muscle from young and old control and Mfn2KO mice and quantification of mitochondrial area and density (n = 3 mice per group). Scale bar: 0.4 μm.

H Representative TEM images of aberrant mitochondria highly present in Mfn2KO old mice.

Data information: Data represent mean ± SEM. $^{\#}P < 0.05$ Mfn2KO vs. control mice, $^{*}P < 0.05$ old vs. young mice.
Source data are available online for this figure.

increased in Mfn2KO old mice compared to controls (Fig 3A) as a result of an increase in adiposity (Fig 3B), with no changes in the weight of liver, heart, or brain (Appendix Fig S2A) and without changes in food intake (Appendix Fig S2B). Moreover, by using indirect calorimetry, we showed that during aging there is a decrease in whole-body oxygen consumption in control mice which is further decreased in Mfn2KO old animals (Fig 3C and D). Activity was also reduced in Mfn2KO old mice in the night-active period (Fig 3E). Glucose oxidation fluxes also decreased during aging in both diurnal and nocturnal phases, and a greater reduction was detected in Mfn2KO mice (Fig 3F). Lipid oxidation in the diurnal phase were equally reduced by aging in both genotypes (Fig 3G). However, lipid oxidation was higher in Mfn2KO animals during the night irrespective of age, indicating a lower suppression of lipid oxidation during the night-feeding period (Fig 3G). This pattern is consistent with the presence of metabolic inflexibility in Mfn2KO mice.

Previously, we reported that 12-month-old Mfn2KO mice showed enhanced susceptibility to develop insulin resistance compared to control animals (Sebastian *et al*, 2012). However, no changes in glucose tolerance or insulin tolerance were detected at that age (Sebastian *et al*, 2012). Here, we extended the study to

 © 2016 The Authors

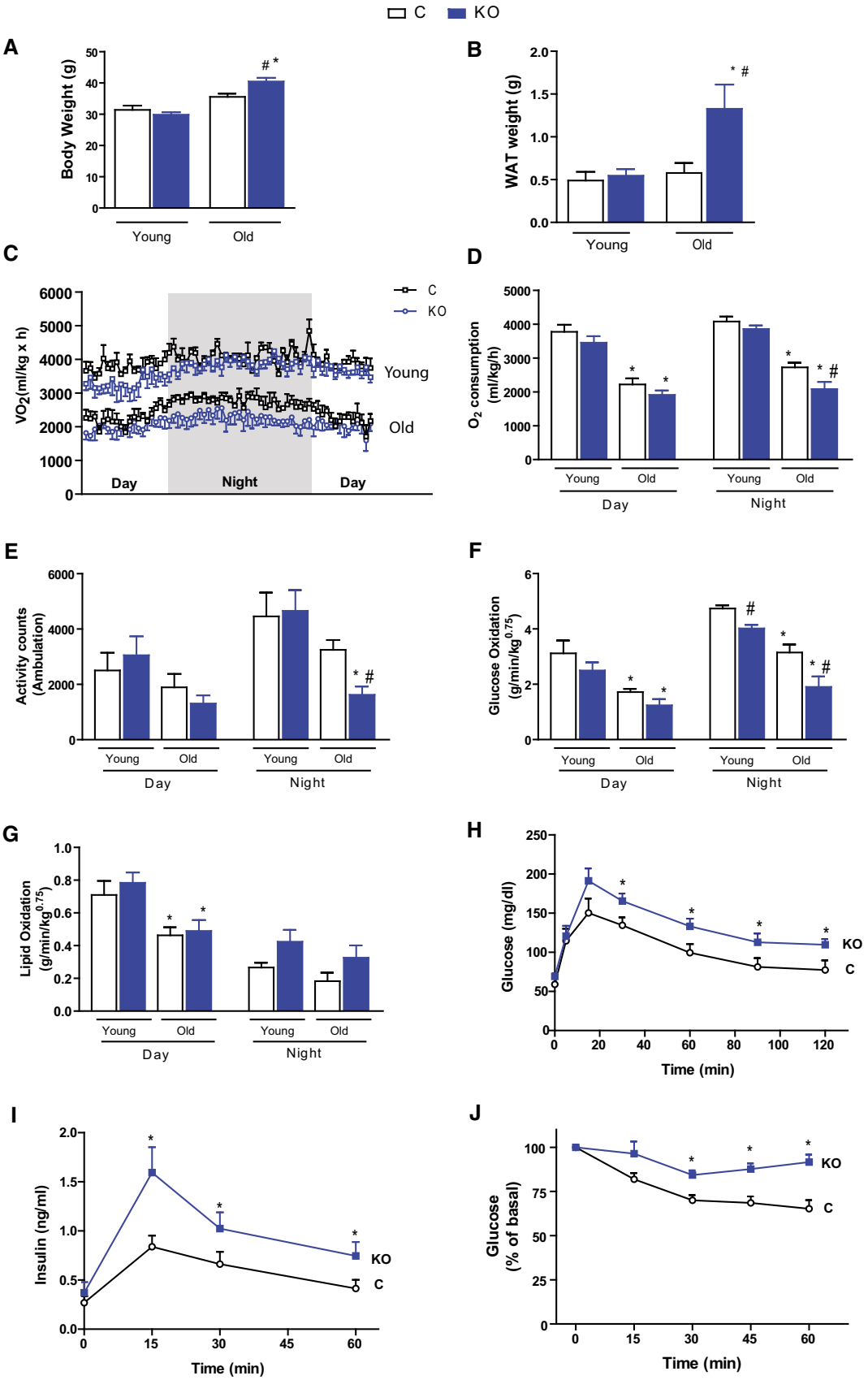

Figure 3.

© 2016 The Authors

Figure 3. Mfn2 deficiency during aging is a contributing factor for age-related metabolic disease.

A Body weight in young and old control and Mfn2KO mice (n = 6 mice per group).
B Epididymal adipose tissue weight in young and old control and Mfn2KO mice (n = 6 mice per group).
C, D Whole-body oxygen consumption was evaluated by indirect calorimetry in young and old control and Mfn2KO mice (n = 6 mice per group).
E Ambulation movement of young and old control and Mfn2KO mice during day and nighttime (n = 6 mice per group).
F, G Glucose (F) and lipid (G) oxidation fluxes expressed as the mean during day and nighttime (n = 6 mice per group).
H Glucose tolerance test (GTT) was performed in control and Mfn2KO old mice (n = 6 mice per group).
I Insulin levels were measured in plasma from control and Mfn2KO old mice subjected to GTT (n = 6 mice per group).
J Insulin tolerance test was performed in control and Mfn2KO old mice (n = 6 mice per group).

Data information: Data represent mean ± SEM. $^{\#}P < 0.05$ Mfn2KO vs. control mice, $^{*}P < 0.05$ old vs. young mice.

22-month-old mice and we found that at this age, Mfn2KO mice were glucose intolerant (Fig 3H), showed greater insulin levels during the glucose tolerance test (Fig 3I) and were profoundly insulin resistant (Fig 3J). Metabolic analysis of 6-, 12-, and 22-month-old mice showed that the impaired metabolic homeostasis (basal insulinemia, insulin levels during the glucose tolerance test, and insulin tolerance test) was gradual during aging, but in Mfn2KO, this process was accelerated (alterations normally seen at 22 months in control mice were already detectable in 12-month-old Mfn2KO mice) (Appendix Fig S2C–E). Basal levels of Akt phosphorylation were reduced in old mice, indicating a lower basal insulin signaling, and AMPK phosphorylation was increased only in old Mfn2KO mice, probably as a result of alterations in the energy status (Appendix Fig S2F). Overall, our results documented that Mfn2 downregulation during aging plays a relevant role in the triggering of age-related metabolic alterations.

Mfn2 deficiency induces muscle atrophy and increases sarcopenia

During aging, there is a gradual loss of muscle mass and function (sarcopenia) (Cesari *et al*, 2014). It has been postulated that mitochondrial dysfunction is a contributing factor, although the mechanisms involved have not yet been elucidated (Marzetti *et al*, 2013). Based on the effects of Mfn2 deficiency on other age-related abnormalities, we analyzed whether Mfn2 could have a role in this process. Muscles from young Mfn2KO showed a moderate reduction in mass (Fig 4A) and a greater reduction in muscle fiber size as assessed by cross-sectional area (CSA) (Fig 4B and C). During aging, there is a reduction in muscle mass in both genotypes, but CSA was lower in old Mfn2KO mice compared to age-matched controls (Fig 4A–C). Analysis of fiber size distribution confirmed these results, showing that aging or Mfn2 deficiency led to an increased number of small fibers and a reduced number of larger fibers (Fig 4C). Further analyses revealed that muscle atrophy in Mfn2-deficient mice and during normal aging was due to the specific atrophy of type IIb glycolytic fibers (Fig 4F). Type IIb represents the majority of fibers in gastrocnemius, and although oxidative fibers are usually smaller than glycolytic fibers (Hamalainen & Pette, 1993), only minor changes in the proportion of fiber types were detected by Mfn2 deficiency in young mice, corresponding to slight increases of type I and IIx fibers (Fig 4D and E).

The increased muscle atrophy in Mfn2KO mice together with the reduced ambulation detected in indirect calorimetry studies (Fig 3E) suggests an impaired muscle function in Mfn2KO old mice. To investigate muscle performance, we performed treadmill and grip strength test in control and Mfn2KO mice. Old Mfn2KO mice showed lower physical capacity, as revealed by a decrease in the total time and distance ran on the treadmill (Fig 4G), which correlated with reduced grip strength (Fig 4H). We next assessed muscle mechanical properties on isolated muscles *ex vivo*. Muscles from old Mfn2KO mice showed a decreased capacity to increase their force after tetanic stimulation compared to the old control group (Fig 4I). Detailed graphical analyses of muscle contraction parameters showed an increase in the twitch to tetanus ratio, half relaxation time and in contraction time in muscles from old Mfn2KO mice (Fig 4J–L). Of note, these parameters have been reported to be altered with aging in both rodents and humans (Campbell *et al*, 1973; Fitts *et al*, 1984; Brooks & Faulkner, 1988). Taken together, our results indicate that Mfn2 deficiency promotes sarcopenia and impairs muscle function during aging.

To further confirm that the muscle alterations were a consequence of a primary deficiency of Mfn2 in skeletal muscle, we generated a new mouse model with a specific ablation of Mfn2 in skeletal muscle (MLC1-Mfn2KO mice or SkM-KO mice). SkM-KO

Figure 4. Reduction in Mfn2 expression induces muscle atrophy and loss of muscular function.

A Gastrocnemius muscle weight in young and old control and Mfn2KO mice (n = 6 mice per group).
B Representative image of hematoxylin and eosin staining in transversal sections of gastrocnemius muscle and quantification of cross-sectional area (CSA) (n = 3 mice per group, 200 fibers per mouse).
C Fiber size distribution in gastrocnemius from young and old control and Mfn2KO mice (n = 3 mice per group, 200 fibers per mouse).
D, E Quantification of fiber type distribution by immunohistochemistry in gastrocnemius muscle from young and old control and Mfn2KO mice (D) and a representative image (E). Fibers were classified as IIa, IIx, IIb, and I (n = 3 mice per group, 200 fibers per mouse).
F Quantification of CSA according to each type of fiber (IIa, IIx, IIb, and I) in gastrocnemius muscle (n = 3 mice per group, 200 fibers per mouse).
G Muscle performance was assessed by measuring the total distance and time ran on a treadmill exhaustion test (n = 6 mice per group).
H Muscle force was assessed measuring grip strength in *in vivo* old mice (n = 6 mice per group).
I–L Muscle force was evaluated in *ex vivo* soleus muscles from old control and Mfn2KO mice. Maximal tetanic force (I), twitch to tetanus ratio (J), half relaxation (K), and contraction times (L) were measured (n = 4 soleus per genotype).

Data information: Data represent mean ± SEM. $^{\#}P < 0.05$ Mfn2KO vs. control mice, $^{*}P < 0.05$ old vs. young mice.

 © 2016 The Authors

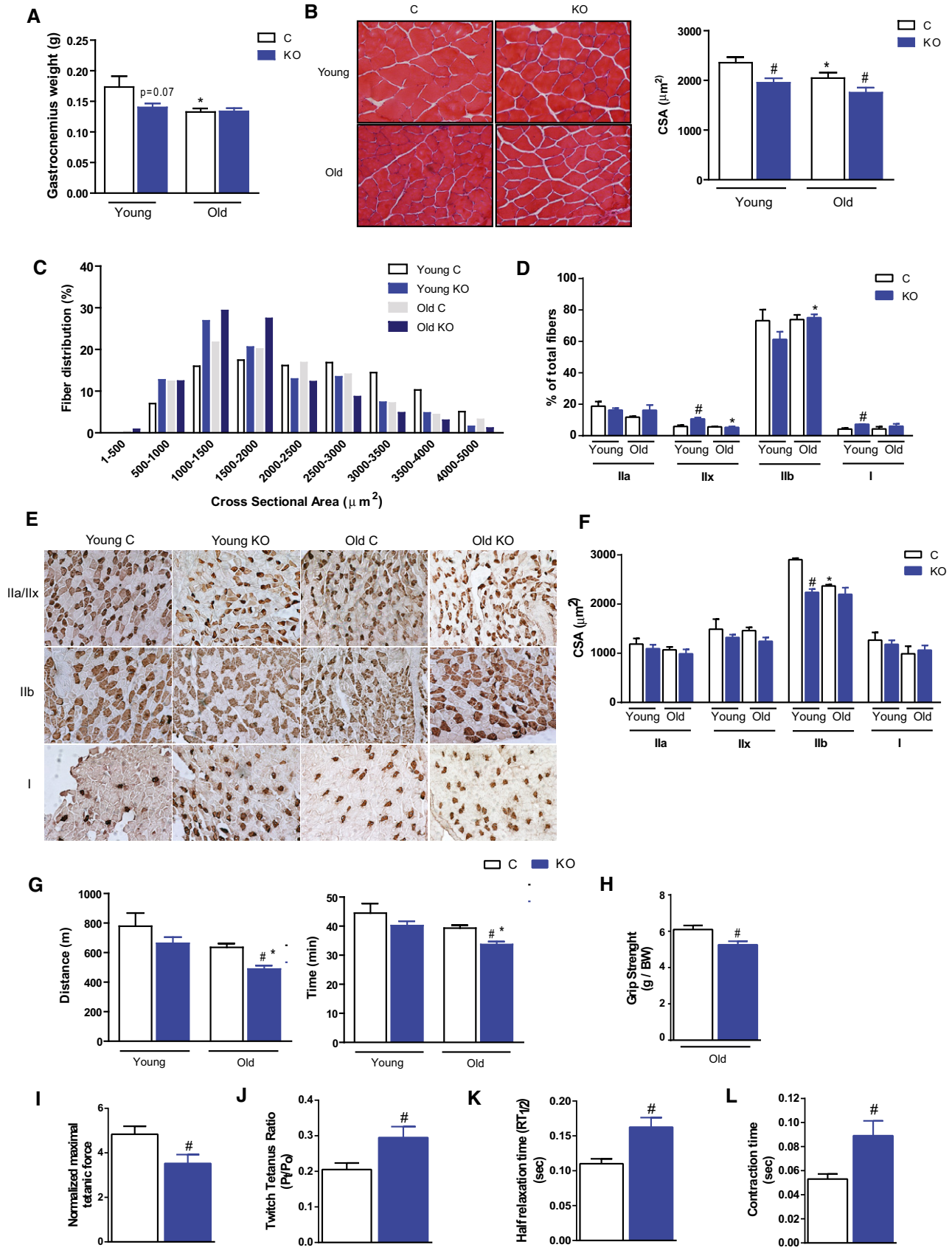
A
Gastrocnemius weight (g)
C
KO
p=0.07
Young
Old
B
C
KO
Young
Old
CSA (μm2)
C
Young C
Young KO
Old C
Old KO
Fiber distribution (%)
1-500
500-1000
1000-1500
1500-2000
2000-2500
2500-3000
3000-3500
3500-4000
4000-5000
Cross Sectional Area (μ m2)
D
% of total fibers
IIa
IIx
IIb
I
E
Young C
Young KO
Old C
Old KO
IIa/IIx
IIb
I
F
CSA (μm2)
G
Distance (m)
Time (min)
H
Grip Strenght (g / BW)
I
Normalized maximal tetanic force
J
Twitch Tetanus Ratio (Pt/Po)
K
Half relaxation time (RT1/2) (sec)
L
Contraction time (sec)

Figure 4.

mice showed a drastic reduction in Mfn2 expression in different muscles whereas no alterations were detected in other tissues (Appendix Fig S3A). As it has been shown for young Mfn2KO mice (Sebastian *et al*, 2012), young SkM-KO mice displayed no alterations in glucose homeostasis (Appendix Fig S3B and C). However, muscle-specific ablation of Mfn2 caused a reduced whole-body oxygen consumption (Appendix Fig S3D). Importantly, young SkM-KO mice also developed muscle atrophy as shown in Mfn2KO mice (Appendix Fig S3E). In all, SkM-KO mice recapitulate the main phenotypic features shown in Mfn2KO mice.

Muscle Mfn2 deficiency during aging causes a reduced mitochondrial autophagy

In order to study the mechanisms by which Mfn2 deficiency develops muscle atrophy and sarcopenia, we evaluated the involvement of relevant pathways. An increased proteasomal protein degradation does not seem to be the cause of muscle atrophy in Mfn2KO mice, as evidenced by the lack of differences between genotypes on the expression of the atrogenes *FbxO32* (atrogin-1), *Murf1, SMART, FbxO31,* and *MUSA1*, in the levels of K48-linked ubiquitinated proteins or in proteasome activity (Fig EV2A–E). Analysis of the mTOR signaling pathway revealed a reduction in phosphorylation of S6 during aging and in Mfn2KO mice with no changes in phosphorylation of 4EBP (Fig EV2F). Consistent with lower S6 phosphorylation, *in vivo* protein synthesis using SUnSET method was clearly reduced in skeletal muscle from Mfn2KO (Fig EV2G).

Macroautophagy (hereafter autophagy) is a key process in the maintenance of tissue quality by removing damaged structures or organelles and protein aggregates. Moreover, an inhibition of autophagy has been shown to be associated with muscle atrophy (Masiero & Sandri, 2010; Carnio *et al*, 2014) and aging (Kroemer, 2015). Mfn2 depletion in cells in culture and heart has been shown to block autophagy (Zhao *et al*, 2012; Munoz *et al*, 2013; Ding *et al*, 2015). Therefore, we analyzed autophagy in control and Mfn2KO mice and we found that aging leads to an increase in mRNA expression of several autophagy markers, such as *LC3b*, *Bnip3*, *Bnip3L* but not *p62*, with no changes between genotypes (Fig EV3A). However, protein expression of LC3II, p62, and BNIP3 was increased during aging and in Mfn2KO mice (Fig 5A–C), suggesting that autophagy was reduced in aged animals but also in Mfn2KO young mice compared to controls. To further confirm the inhibition of autophagy in Mfn2KO mice, we performed autophagy flux analysis by treating mice for 5 days with chloroquine. Indeed, autophagy flux was inhibited in skeletal muscle from Mfn2KO mice (Fig 5D). In order to show that this effect was cell autonomous, we also performed autophagy flux analysis in control and Mfn2KD C2C12 muscle cells. Although no changes were detected for LC3II, autophagy flux was inhibited for p62, NBR1, and BNIP3, indicating a more compromised flux of selective autophagy upon Mfn2 deficiency in muscle cells (Fig EV3B).

By using transmission electron microscopy, we detected the accumulation of autophagosomes in Mfn2KO young mice and control aged animals compared to control young mice, which was again consistent with reduced autophagy (Fig 5E). In Mfn2KO old animals, there was a much greater accumulation of autophagosomes and mitophagosomes (Fig 5E), probably due to the reduced autophagy since early life. Similar alterations were also observed in Mfn2KD C2C12 myotubes by electron microscopy (Fig 5F). The accumulation of mitochondria inside autophagosomes and the increased expression of BNIP3 suggest that mitochondrial autophagy could be also affected by Mfn2 deficiency. Moreover, Mfn2 has been shown to participate in mitophagy in cardiomyocytes (Chen & Dorn, 2013; Song *et al*, 2015). To evaluate this possibility, we obtained mitochondrial fractions from control and Mfn2KD C2C12 myotubes and measured the presence of proteins involved in mitochondrial autophagy. Mfn2KD cells showed increased levels of BNIP3, LC3II, and Parkin in mitochondria (Fig 5G). These data, together with the accumulation of mitophagosomes, suggest that autophagic degradation of mitochondria is impaired in Mfn2KD cells. Treatment of control cells with mitophagy inducer CCCP produced a time-dependent increase in the recruitment of BNIP3, LC3II, and Parkin into mitochondria (Fig 5G). However, in Mfn2KD cells, this recruitment was blocked or decreased. Mitophagic flux was also inhibited *in vivo* in skeletal muscle, as suggested by the lower accumulation of LC3II, p62 and BNIP3 in mitochondrial fractions after treatment with chloroquine (Fig EV3C). Furthermore, despite increased accumulation of mitophagic proteins in mitochondria, mitochondrial mass in Mfn2KD cells (Fig EV3D) and skeletal muscle (Fig 2B) was not decreased.

In all, these data indicate that deficiency of Mfn2 impairs autophagic degradation of mitochondria leading to muscle atrophy. To confirm that inhibition of autophagy is the driver of the muscle atrophy observed in conditions of Mfn2 deficiency, we blocked

Figure 5. Reduction in Mfn2 during aging is associated with a reduction in mitochondrial autophagy in skeletal muscle.

A–C LC3I and LC3II (A), p62 (B), and BNIP3 (C) protein expression was measured in gastrocnemius muscle from young and old control and Mfn2KO mice (n = 4–6 mice per group). LC3II/LC3I ratio was also calculated. Data were normalized by tubulin and expressed as a fold change compared to young control mice.

D Autophagic flux was evaluated in gastrocnemius muscle by treating control and Mfn2KO young mice with chloroquine for five days. LC3, p62, and BNIP3 expression was measured (n = 4–5 mice per group).

E Representative TEM images of quadriceps muscle from Mfn2KO young mice, control old mice and Mfn2KO old mice showing the presence of autophagosomes and mitophagosomes (n = 3 mice per group). Scale bar: 500 nm.

F Representative TEM images of control and Mfn2KD C2C12 myotubes showing the accumulation of autophagosomes upon Mfn2 deficiency (n = 3 independent experiments). Scale bar: 2 μm.

G Presence of autophagic proteins (BNIP3, LC3 and Parkin) on mitochondrial-enriched fractions obtained from control and Mfn2KD C2C12 myotubes untreated or treated with CCCP (n = 3 independent experiments). Data were normalized by TIM44 as a loading control and expressed as a fold change compared to young control mice.

Data information: Data represent mean ± SEM. $^{\#}P < 0.05$ Mfn2KO vs. control mice or Mfn2KD vs. control cells, $^{*}P < 0.05$ old vs. young mice or treated vs. untreated cells.
Source data are available online for this figure.

 © 2016 The Authors

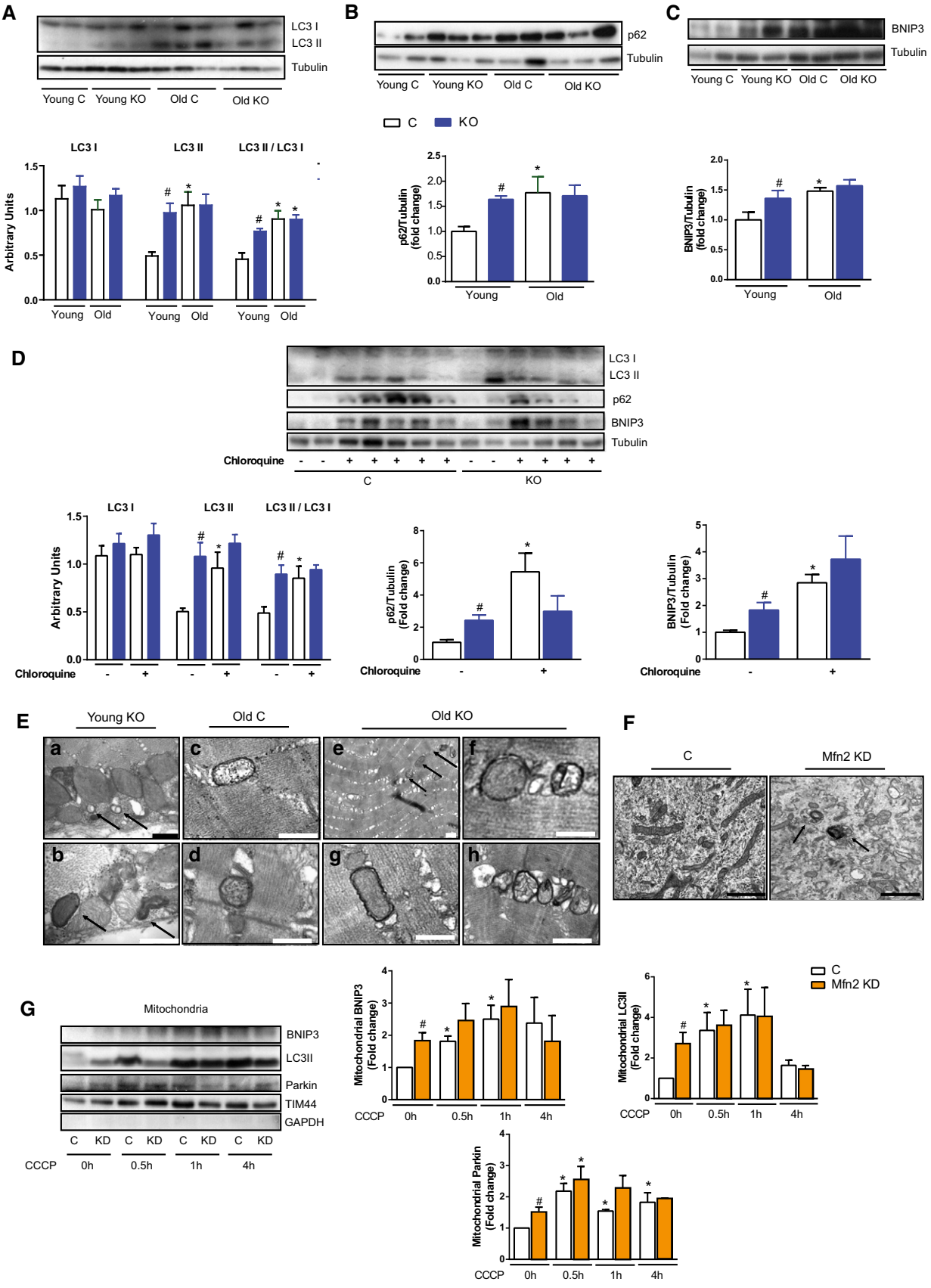

Figure 5.

© 2016 The Authors

autophagy in mouse *in vivo* by injecting chloroquine for 5 days. Administration of chloroquine in mice reduced CSA of gastrocnemius muscle, indicating muscle atrophy (Fig EV3E). However, treatment of Mfn2KO mice with chloroquine did not further reduce CSA compared to control mice (Fig EV3E). In order to stablish a specific role of Mfn2 in reduction in autophagy and muscle atrophy, we performed rescue studies by adenovirus-mediated overexpression of Mfn2 in gastrocnemius muscle from Mfn2KO mice. Re-expression of Mfn2 for 2 weeks led to the restoration of Mfn2 protein levels in skeletal muscle from Mfn2KO mice (Fig EV3F), caused a decrease in the accumulation of autophagy markers and increased CSA values (Fig EV3G and H). These results indicate that reduction in Mfn2 is the underlying mechanism leading to inhibition of autophagy and muscle atrophy.

Mfn2 deficiency triggers a mitochondrial retrograde signaling pathway through the HIF1α transcription factor to induce mitochondrial autophagy

Further GSEA analysis of transcriptomics data from Mfn2KO mice was performed using the curated list of genesets included in the Broad Institute Molecular Signature Database (MsigDB-C2) to find molecular pathways coordinately altered in both Mfn2 deficiency and in normal aging. The use of this approach revealed an enrichment of genesets related with "response to hypoxia" (Fig 6A). In keeping with this, we found that HIF1α, the main regulator of hypoxia response, was upregulated during normal aging and in Mfn2KO mice (Fig 6B). Moreover, we measured the expression of HIF1α target genes, such as *Pdk1*, *Pdk4,* and *Vegfa*, and all of them were upregulated in skeletal muscle of old control and young Mfn2KO mice (Fig EV4A), confirming that HIF1α activity is increased. Similar results were obtained after Mfn2 knockdown in C2C12 myotubes (Figs 6C and EV4B). HIF1α has been described to be involved in the activation of mitochondrial autophagy by upregulating BNIP3 (Zhang *et al*, 2008; Bellot *et al*, 2009). In order to understand the precise role of HIF1α upon Mfn2 deficiency, we evaluated the impact of its increase on BNIP3 expression. To this end, control and Mfn2KD C2C12 myotubes were incubated with the specific HIF1α inhibitor NSC-134754 (Chau *et al*, 2005). As shown in Fig 6C, the increase in HIF1α seen in Mfn2KD myotubes was markedly reduced upon treatment with NSC-134754, which also led to the reduction in BNIP3. We next evaluated whether inhibition of HIF1α and reduction in BNIP3 could affect mitochondrial quality. Analysis of oxidative stress revealed that treatment with HIF1α inhibitor increased the levels of hydrogen peroxide, in both control and Mfn2KD cells (Fig 6D). Moreover, coupled mitochondrial respiration and leak were markedly impaired after treatment with NSC-134754 in Mfn2KD cells (Fig 6E and F). Moreover, mitochondria from Mfn2-deficient cells showed an enhanced abundance of BNIP3, LC3 II, and Parkin, consistent with an adaptive process aimed to mitigate mitochondrial autophagy disruption (Fig 6G). After treatment with HIF1α inhibitor, Mfn2-deficient cells no longer showed an increase in mitochondrial BNIP3 whereas LC3II and Parkin accumulated in mitochondria from control and Mfn2KD myotubes. Our data are coherent with the existence of a further inhibition of mitochondrial autophagy upon HIF1α inhibition. In keeping with this, electron microscopy analysis of control and Mfn2KD cells treated with NSC-134754 showed an increase in the presence of autophagosomes and altered mitochondria, which was much more evident in Mfn2KD cells (Fig 6H and I). These data suggest that Mfn2-induced HIF1α activation constitutes an adaptive mechanism in order to increase BNIP3 expression and removal of damaged mitochondria.

In order to assess whether the decrease in autophagy is a driver of Mfn2 deficiency effects, we used autophagy inhibitor bafilomycin A. Treatment of C2C12 myotubes with bafilomycin A caused a substantial accumulation of BNIP3, LC3II, and Parkin in mitochondrial fractions, as an expected consequence of mitochondrial autophagy inhibition (Fig EV4D). In addition, mitochondrial respiration was profoundly impaired and ROS levels were highly increased, suggesting the accumulation of damaged mitochondria (Fig EV4E–G). Under these conditions, the HIF1α-BNIP3 pathway was also induced (Fig EV4H). Altogether, our results indicate that aging and Mfn2 deficiency and the concomitant reduced mitochondrial autophagy, trigger a mitochondrial retrograde signaling through HIF1α in order to increase the BNIP3-dependent degradation of mitochondria and minimize the accumulation of damaged mitochondria.

The HIF1α-BNIP3 pathway induced by Mfn2 deficiency is ROS-dependent

Next, we analyzed the mechanisms by which aging and Mfn2 deficiency lead to activation of HIF1α. We focused our attention on oxidative stress since ROS has been shown to activate HIF1α in several cell models (Patten *et al*, 2010) and we have shown an enhanced oxidative stress in old control and Mfn2KO mice (Fig 2E). To assess whether ROS has a role in the activation of HIF1α, we treated Mfn2KO and control mice with the antioxidant compound N-acetylcysteine (NAC) for three weeks. NAC treatment of Mfn2KO mice reduced H_2O_2 levels in skeletal muscle (Fig EV5A) and blocked the activation of HIF1α and the increase in BNIP3 (Fig 7A), demonstrating that the increase in the HIF1α-BNIP3 pathway is ROS-dependent. NAC treatment also blocked the increase in ROS and the HIF1α-BNIP3 pathway in C2C12 Mfn2KD myotubes (Fig EV5B and C). These results suggest a beneficial role of ROS as signaling molecules under Mfn2 deficiency conditions. If this was the case, blocking the increase in ROS should exacerbate mitochondrial alterations. In keeping with this, NAC treatment of control and Mfn2 KD C2C12 myotubes increased mitochondrial dysfunction, as demonstrated by a reduced coupled respiration in Mfn2 KD cells (Fig 7B), despite increasing the presence of LC3II and Parkin in mitochondrial fractions in both mice and cells, which is consistent with a further inhibition of mitochondrial autophagy (Fig 7C and D). Autophagic flux was also inhibited by NAC both in control and Mfn2KD cells, suggesting that some ROS is necessary for the maintenance of basal autophagy (Fig EV5D). Accordingly, electron microscopy analysis revealed an increase in autophagosome/mitophagosome accumulation and mitochondrial alterations upon treatment with NAC, which were much more evident in Mfn2 KD cells (Fig 7E). NAC treatment led to a reduction in muscle CSA in control mice (Fig EV5E), in keeping with reduced autophagy. The reduction in muscle fiber size was greater in Mfn2KO mice, highlighting the importance of the ROS-dependent adaptive increase in BNIP3-driven mitochondrial autophagy under Mfn2-deficient conditions (Fig EV5E). Overall, these results indicate that aging and Mfn2 deficiency induce a retrograde signaling pathway through a ROS-dependent activation of HIF1α in order to mitigate the defective mitochondrial autophagy.

 © 2016 The Authors

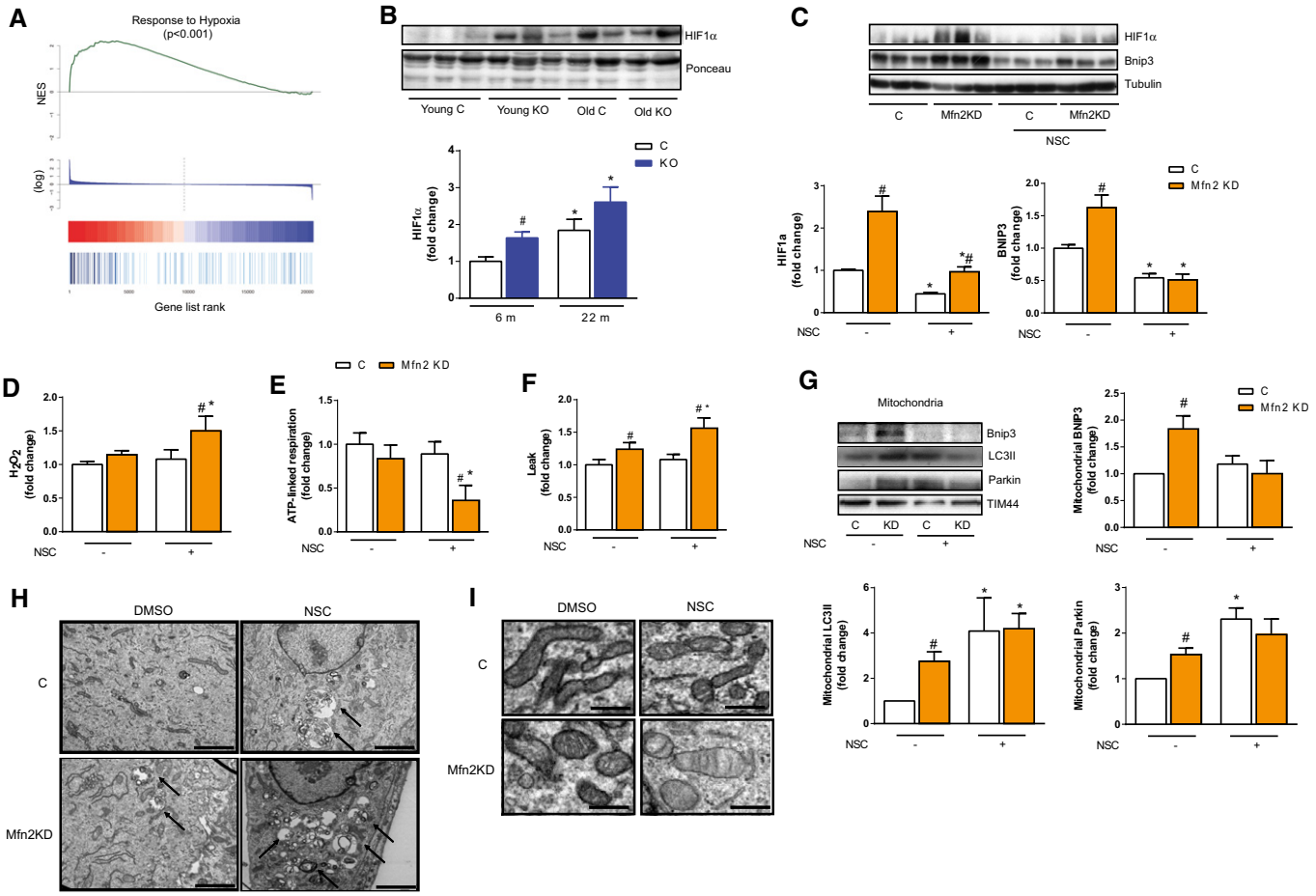

Figure 6. Mfn2 deficiency triggers a retrograde signaling pathway involving HIF1α in order to promote mitochondrial autophagy and minimize mitochondrial damage.

A GSEA plot using BroadC2 database showed that genes differentially expressed in young control compared to young Mfn2KO mice and old control mice are enriched in genes related to hypoxia response.

B HIF1α protein expression was measured in nuclear extracts from young and old control and Mfn2KO mice (n = 4–6 mice per group). Data were normalized by tubulin as a loading control and expressed as a fold change compared to young control mice.

C HIF1α and BNIP3 protein expression were measured in control and Mfn2KD C2C12 myotubes untreated or treated with the HIF1α-specific inhibitor NSC-134754 (n = 3 independent experiments performed in triplicate). Data were normalized by tubulin as a loading control and expressed as a fold change compared to control C2C12 myotubes.

D Levels of H_2O_2 were measured in control and Mfn2KD C2C12 myotubes untreated or treated with NSC-134754 (n = 5 independent experiments performed in duplicate). Data were expressed as a fold change compared to control C2C12 myotubes.

E, F Respiration was measured in control and Mfn2KD C2C12 myotubes untreated or treated with NSC-134754 and ATP-coupled respiration (E) and proton leak (F) were calculated (n = 8 independent experiments). Data were expressed as a fold change compared to control C2C12 myotubes.

G Autophagic protein abundance (BNIP3, LC3II, and Parkin) was measured in mitochondrial-enriched fractions from control and Mfn2KD C2C12 myotubes untreated or treated with NSC-134754 (n = 4 independent experiments). Data were normalized by TIM44 as a loading control and expressed as a fold change compared to control C2C12 myotubes.

H, I Representative TEM images of control and Mfn2KD C2C12 myotubes untreated or treated with NSC-134754 showing the accumulation of autophagosomes (H, arrows) and the presence of mitochondrial alterations (I) in Mfn2KD or NSC-134754-treated cells. Scale bar: 2 μm.

Data information: Data represent mean ± SEM. $^{\#}P < 0.05$ Mfn2KO vs. control mice or Mfn2KD vs. control cells, $^{*}P < 0.05$ old vs. young mice or treated vs. untreated cells.
Source data are available online for this figure.

Discussion

In the present study, we have demonstrated the involvement of the mitochondrial fusion protein mitofusin 2 in the aging process. Mfn2 repression in muscle during aging is a determinant for the inhibition of autophagy and accumulation of damaged mitochondria, and contributes to age-associated metabolic alterations and sarcopenia. In addition, Mfn2 deficiency triggers an adaptive pathway in order to mitigate mitochondrial damage. These conclusions are based on a number of outstanding observations, namely: (i) normal aging is characterized by a progressive reduction in Mfn2 expression in skeletal muscle; (ii) skeletal

© 2016 The Authors

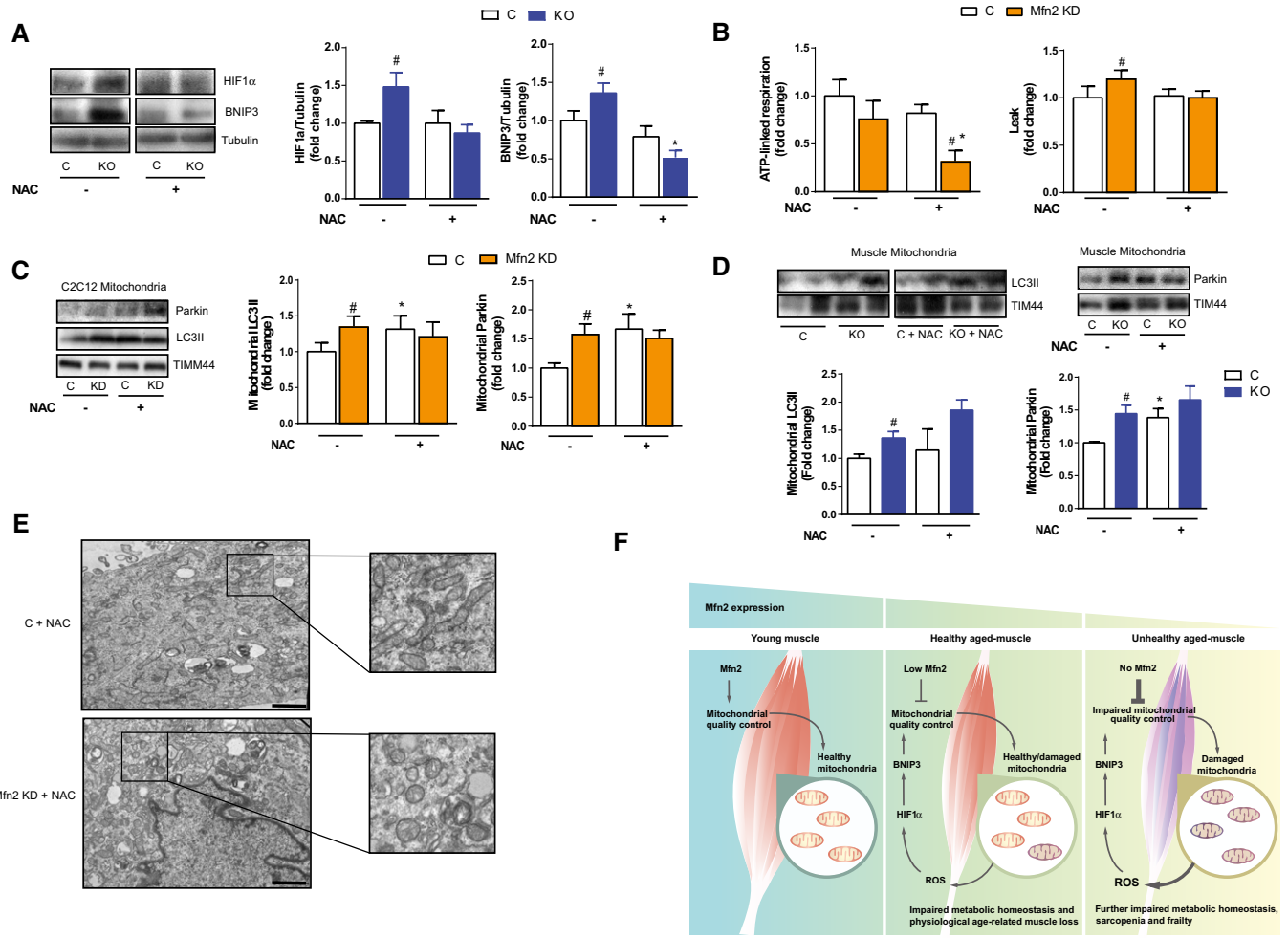

Figure 7. Mfn2-induced HIF1α retrograde signaling pathway is dependent on ROS signaling.

A HIF1α and BNIP3 protein expression was measured in gastrocnemius muscle from control and Mfn2KO young mice untreated or treated with NAC (n = 3–5 mice per group). Data were normalized by tubulin as a loading control and expressed as a fold change compared to young control mice.

B Respiration was evaluated in control and Mfn2KD C2C12 myotubes untreated or treated with NAC. ATP-coupled respiration (left panel) and proton leak (right panel) were calculated (n = 5 independent experiments). Data were expressed as a fold change compared to control C2C12 myotubes.

C Expression of LC3II and Parkin was evaluated in mitochondrial-enriched fractions from control and Mfn2KD C2C12 myotubes untreated or treated with NAC (n = 5 independent experiments). Data were normalized by TIM44 as a loading control and expressed as a fold change compared to control C2C12 myotubes.

D Expression of LC3II and Parkin was evaluated in mitochondrial-enriched fractions in gastrocnemius muscle from control and Mfn2KO mice untreated or treated with NAC (n = 5 mice per group). Data were normalized by TIM44 as a loading control and expressed as a fold change compared to young control mice.

E Representative TEM images of control and Mfn2KD C2C12 myotubes treated with NAC showing increased number of autophagosomes and mitochondrial alterations (n = 3 independent experiments). Scale bar: 2 μm.

F Proposed model for the role of Mfn2 during aging in skeletal muscle.

Data information: Data represent mean ± SEM. $^{\#}P < 0.05$ Mfn2KO vs. control mice or Mfn2KD vs. control cells, $^{*}P < 0.05$ old vs. young mice or treated vs. untreated cells.
Source data are available online for this figure.

muscle Mfn2 deficiency in mice generates a genetic signature common to normal aging, indicating that both conditions show common regulators; (iii) muscle Mfn2 deficiency is characterized by further impairment in age-related alterations; (iv) muscle Mfn2 ablation caused impaired mitochondrial quality control, leading to the accumulation of dysfunctional mitochondria; and (v) accumulation of damaged mitochondria induced by Mfn2 deficiency triggered a ROS-dependent increase in HIF1α and BNIP3 which promoted mitochondrial autophagy. These alterations caused by Mfn2 ablation occurred without affecting life span. Overall, our results allow us to propose that Mfn2 is a key protein that maintains mitochondrial quality and function, and therefore, its repression causes accelerated aging. Although a possible role of mitochondrial dynamics proteins in aging and longevity has been suggested in model organisms such as yeast (Scheckhuber *et al*, 2007; Bernhardt *et al*, 2015) and *C. elegans* (Yang *et al*, 2011), to our knowledge, this is the first report establishing a direct connection between a protein involved in mitochondrial dynamics and

 © 2016 The Authors

aging in mammals. In addition, our data are consistent with data indicating that aging is linked to defective mitophagy in *C. elegans* (Artal-Sanz & Tavernarakis, 2009; Palikaras *et al*, 2015).

We report that aging is characterized by a marked repression of Mfn2 protein in mouse muscle, probably as a consequence of either a lower rate of Mfn2 mRNA translation or a reduced protein stability. This occurs under conditions in which other mitochondrial dynamics proteins are also decreased but other mitochondrial proteins such as porin or OXPHOS subunits are not altered, indicating a specific dysregulation of mitochondrial dynamics during aging. Reduction in Mfn2 found in our study is consistent with other reports in humans or rats in which Mfn2 was found to be downregulated during aging in skeletal muscle (Crane *et al*, 2010; Zhao *et al*, 2014). It has also been reported that Mfn2 expression is not altered in the white portion of gastrocnemius muscles in aged mice (Leduc-Gaudet *et al*, 2015). In this context, the expression of Mfn2 is greater in oxidative than glycolytic muscles (F.X. Soriano and A. Zorzano, unpublished observations). Based on all these data, we claim that most likely Mfn2 is mostly repressed in highly oxidative muscle fibers during aging, as shown by a higher repression in soleus than in tibialis anterior muscle (Fig EV1A). In keeping with a reduced Mfn2 expression in aged muscle, by means of transcriptomics analysis, we have identified a muscle gene signature that is common in normal aging as well as in Mfn2 deficiency. Thus, Mfn2-deficient muscle showed a pattern of deregulated genes also noted in muscles from aged mice. These data support the view that Mfn2 repression during aging potently influences muscle biology.

Skeletal muscle tissue is highly affected during aging, and this has relevant consequences on muscle mass (sarcopenia), capacity to perform work, and on energy homeostasis (Dela & Kjaer, 2006; Cesari *et al*, 2014). The mechanisms leading to age-induced muscle alterations are not known, and mitochondrial dysfunction has been suggested to be a possible cause (Lanza & Nair, 2010; Marzetti *et al*, 2013). Here, we show that normal aging in mice is characterized by mitochondrial dysfunction, reduction in mitochondrial density, and accumulation of altered mitochondria, as evidenced in previous reports (Shigenaga *et al*, 1994; Ojaimi *et al*, 1999; Short *et al*, 2005). Aging also caused glucose intolerance, reduced energy expenditure, and reduced muscle fiber size. Importantly, muscle Mfn2 ablation aggravated all these age-related disorders. Based on these observations, we suggest that age-induced decay in Mfn2 in skeletal muscle could be a contributing factor for the mitochondrial and metabolic alterations linked to aging. In addition, we suggest that an exaggerated Mfn2 repression in muscle with aging may be linked to unhealthy aging, and it may favor the development of the frailty syndrome.

Autophagy is reduced during aging (Salminen & Kaarniranta, 2009; Carnio *et al*, 2014), and its involvement in the accumulation of tissue damage occurring with age has been suggested (Kroemer, 2015). Autophagy is also essential for the maintenance of skeletal muscle mass and function as well as whole-body energy homeostasis (Masiero *et al*, 2009; Masiero & Sandri, 2010). In keeping with this, we showed that aging in control mice is associated with a decrease in autophagy and with an increased abundance of abnormal mitochondria. Mfn2 deficiency also reduced autophagy in skeletal muscle and muscle cells in culture, demonstrating a cell autonomous effect of Mfn2 repression. Analysis of autophagy flux in muscle cells suggests that selective autophagy (which requires the adaptor proteins p62, BNIP3, and NBR1) is more affected by Mfn2 deficiency than general non-selective autophagy. Furthermore, Mfn2 repression also inhibited autophagic degradation of mitochondria in skeletal muscle and muscle cells in culture, leading to an extended presence of abnormal mitochondria, which correlated with an enhanced oxidative stress. These data indicate a role for Mfn2 downregulation as the cause underlying the decrease of mitochondrial autophagy occurring with age in skeletal muscle. These results are consistent with previous studies demonstrating a role of Mfn2 in autophagy and mitophagy (Hailey *et al*, 2010; Zhao *et al*, 2012; Chen & Dorn, 2013; Munoz *et al*, 2013; Song *et al*, 2015) and a role of mitochondrial dynamics in mitochondrial quality control (Twig *et al*, 2008). Moreover, disruption of mitochondrial dynamics has also been shown to be associated with muscle atrophy (Romanello *et al*, 2010). Therefore, we suggest that Mfn2 repression during aging leads to alterations in autophagy and to an inhibition of mitochondrial quality control, contributing to the accumulation of damaged mitochondria and muscle atrophy. In keeping with this, re-expression of Mfn2 in skeletal muscle from Mfn2KO mice restored autophagy and reversed muscle atrophy.

It is likely that inhibition of autophagy actively participates in many of the alterations detected under muscle Mfn2 deficiency conditions. In this context, treatment of mice with autophagy inhibitor chloroquine caused muscle atrophy as noted by reduced muscle fiber size. Similarly, treatment of muscle cells with autophagy inhibitor bafilomycin A1 caused enhanced ROS production and mitochondrial dysfunction. All these data are coherent with the model that muscle Mfn2 repression driven by aging reduces mitochondrial autophagy, which in turn leads to mitochondrial dysfunction and other downstream events such as muscle atrophy or alterations in nutrient handling.

Surprisingly, we have documented that both normal aging and Mfn2 deficiency cause a mitochondrial retrograde signaling through induction of HIF-1α in skeletal muscle. This is a cell autonomous response also detectable in cultured muscle cells upon Mfn2 deficiency. HIF1α has been shown to have a role in the activation of mitochondrial autophagy by upregulating BNIP3 (Zhang *et al*, 2008; Bellot *et al*, 2009). Activation of this pathway involves the induction of BNIP3 and the potentiation of autophagic degradation of mitochondria, thereby minimizing accumulation of damaged mitochondria. Blocking this pathway by a specific HIF1α inhibitor leads to increased mitochondrial damage and metabolic collapse. Moreover, we found that the increase in HIF1α was ROS-dependent, as treatment of mice or muscle cells with the antioxidant NAC blocked the increase in HIF1α and BNIP3, leading to an increased abundance of damaged mitochondria and reduced mitochondrial metabolism, revealing the importance of the HIF1α retrograde signaling in cell homeostasis. In addition, NAC treatment worsened muscle atrophy in Mfn2KO mice, highlighting the importance of this adaptive pathway in minimizing muscle damage. Blockage of mitochondrial autophagy induced with bafilomycin A1 also led to accumulation of damaged mitochondria, an increase in ROS production, and activation of the HIF1α-BNIP3 pathway. These data strongly suggest that inhibition of mitochondrial quality control and accumulation of damaged mitochondria is the driver of the activation of the HIF-1α adaptive retrograde signaling. In keeping with this, a similar adaptive pathway involving ROS-induced increase in NRF2 and

© 2016 The Authors

BNIP3 has been recently shown to be activated by accumulation of damaged mitochondria during aging in *C. elegans* (Palikaras *et al*, 2015), although the mechanisms by which aging leads to accumulation of mitochondrial damage have not been analyzed. Here, we propose that the decrease of Mfn2 could be the link between aging and accumulation of damaged mitochondria. Although HIF1α has been shown to increase during aging affecting nuclear–mitochondrial communication (Gomes *et al*, 2013), here we discovered a different and previously unknown retrograde signaling pathway triggered by aging-induced Mfn2 downregulation, which is formed by HIF1α-BNIP3 in order to minimize mitochondrial damage and muscle atrophy during aging.

In summary, we propose a model (Fig 7F) in which Mfn2 controls the optimal biological properties of skeletal muscle through the maintenance of mitochondrial quality control and efficient mitochondrial metabolism. During normal aging, skeletal muscle undergoes Mfn2 repression, which causes a reduction in mitochondrial autophagy and therefore a reduction in mitochondrial metabolism resulting in an increase of damaged mitochondria, which leads to an increase in ROS production. Ablation of Mfn2 reproduces those alterations in young mice and aggravates them in old mice, strongly supporting a role for muscle Mfn2 in aging. Surprisingly, the alterations in mitochondrial function induce a mitochondrial retrograde signaling through HIF-1α, enhanced BNIP3, contributing to the maintenance of mitochondrial autophagy. We also suggest that conditions characterized by extremely reduced muscle Mfn2 are bound to unhealthy aging. Under these conditions, mitochondrial autophagy undergoes a further impairment and leads to the occurrence of more extensive mitochondrial damage. This situation, taken as a whole, causes metabolic alterations linked to an impairment of metabolic homeostasis and low energy expenditure, sarcopenia, and reduced muscle performance. Overall, the data presented here strongly support the view that Mfn2 constitutes a novel target for the treatment of age-related alterations in skeletal muscle.

Materials and Methods

Refer to Appendix Supplementary Methods for a detailed description of all methods used.

Animal care and generation of Mfn2KO mice

All animal work was conducted according to guidelines established by the Parc Científic de Barcelona and the University of Barcelona Committees on Animal Care. For aging studies, wild-type mice were used at 6, 12, and 22 months of age. Mef2C-Cre$^{+/-}$Mfn2$^{LoxP/LoxP}$ mice (Mfn2KO mice) were obtained as described (Sebastian *et al*, 2012) by crossing Mfn2$^{flox/flox}$ mice, provided by Dr. David Chan (Mfn2^{tm3Dcc}/Mmcd) (Chen *et al*, 2007) through MMRRC and a mouse strain expressing Cre recombinase under the control of skeletal muscle-specific promoter from MEF2C (mef2-73k-Cre) (Heidt & Black, 2005). MLC1-Cre$^{+/-}$Mfn2$^{LoxP/LoxP}$ mice (SkM-KO mice) were obtaining by crossing Mfn2$^{flox/flox}$ mice and a mouse strain expressing Cre recombinase under the control of MLC1 promoter/enhancer (Sala *et al*, 2014). Non-expressing Cre littermates were used as control mice.

Cell culture and treatments and adenoviral transduction

C2C12 myoblasts were used in this study. C2C12 myoblasts were grown and led to differentiate into myotubes as previously described (Canto *et al*, 2007). C2C12 myotubes were transduced with Ad-miRCt (encoding for a control microRNA) and Ad-miR2 (encoding for five different microRNAs against Mfn2) adenovirus (Sebastian *et al*, 2012) for 48 h at day 4 of differentiation at multiplicity of infection of 200 pfu/cell. All the experiments were performed 48 h after infection. C2C12 myotubes were incubated with NSC-134754 (10 μM) or N-acetylcysteine (5 mM) for 16 h. CCCP was used at 30 μM for 0.5, 1, and 4 h and bafilomycin A at 200 nM for 3 or 16 h.

In vivo metabolic measurements

Serum samples were taken between 10 and 12 am after an overnight fast, or at the same time in fed conditions. Blood glucose was assayed with an Accu-Chek glucose monitor (Roche Diagnostics Corp.). Glucose and insulin tolerance tests were performed. Insulin concentration was also measured.

Evaluation of muscle force and performance

Maximal muscle strength of forelimbs was measured using a grip strength meter (Bioseb). Muscle mechanical properties *ex vivo* as described previously (Pessina *et al*, 2014) were quantified with the commercially available 1200 A isolated muscle test system (Aurora Scientific Inc., ON, Canada). Muscle performance was evaluated by an exhaustion protocol using a treadmill.

Assessment of oxygen consumption in mouse by indirect calorimetry

Measurements of oxygen consumption (VO_2) and CO_2 production (VCO_2) were performed using an indirect calorimetry system (Oxymax, Columbus Instruments).

Respiration measurements in permeabilized muscle fibers, isolated mitochondria, and muscle cells

Respiration of permeabilized muscle fibers, mitochondria, and cultured cells was measured as described in Sebastian *et al* (2012).

Histological sample preparation and analysis

For light microscopy, muscles were removed, embedded in OCT solution (TissueTek), immediately frozen in liquid nitrogen-cooled isopentane (Sigma), and stored at −80°C. About 10 μm cryosections of gastrocnemius muscles were used. Cryosections were stained with hematoxylin and eosin following standard protocols to check tissue architecture and CSA. CSA was quantified in 200 fibers/mouse using Image J software. NADH diaphorase and SDH activity staining on cryosections was performed as described (Sala *et al*, 2014). Sequential COX/SDH staining was performed as described in (Ross, 2011). A Nikon E600 equipped with the Olympus DP 72 camera microscope was used to analyze light and fluorescence cryosection staining. Acquisition software used was Cell F from Olympus.

 © 2016 The Authors

Fiber typing in muscle sections

Serial gastrocnemius cryosections were obtained and examined by standard immunohistochemical procedures for the expression of myosin heavy chain (MHC) isoforms (Serrano *et al*, 2001) as described (Sala *et al*, 2014).

Protein extraction and Western blotting

Skeletal muscle or cultured cells protein homogenates, mitochondrial and nuclear fractions were used for Western blotting. For detailed methods and antibodies used, see Appendix Supplementary Methods.

Measurement of *in vivo* protein synthesis

For *in vivo* protein synthesis determination, SUnSET methodology was used (Goodman *et al*, 2011). Briefly, mice were anesthetized with an intraperitoneal injection of ketamine (100 mg/kg) and xylazine (10 mg/kg) and then given an intraperitoneal injection of 0.04 μmol/g puromycin dissolved in 100 μl of PBS. 30 min after injection, tissues were extracted and frozen in liquid N_2 for WB analysis.

Proteasome activity

Proteasome activity in total homogenates from gastrocnemius muscles was measured as reported (Strucksberg *et al*, 2010).

Isolation of polysomal fractions from skeletal muscle

Polysomal fractions were obtained from quadriceps muscle as described (Williamson *et al*, 2006) with minor modifications. About 200 mg of muscle was homogenized in 1 ml of resuspension buffer (50 mM Hepes pH 7.4; 75 mM KCl, 5 mM $MgCl_2$, 250 mM sucrose, 1% Triton X-100, 1.3% deoxycholate, 100 μg/ml cycloheximide, and 25 μl ribonuclease inhibitor SUPERasin per 5 ml buffer). Homogenates were incubated for 5 min on ice, and then, 150 μl of Tween–deoxycholate mix (1.34 ml Tween 20, 0.66 g deoxycholate, 18 ml sterile water) was added and incubated for 15 min on ice. Homogenate was centrifuged at 1,000 *g* for 15 min. The resulting supernatant was loaded onto a 20% (w/v) sucrose cushion (1:1 homogenate:sucrose cushion) and centrifuged at 150,000 *g* for 2 h. The ribosome-containing pellet (polysomes) was collected and used for RNA extraction.

DNA and RNA extraction and real-time PCR

Mice were sacrificed by cervical dislocation, and tissues were immediately frozen for RNA and DNA isolation. RNA samples from tissues or polysomal fractions were extracted and reverse-transcribed as described (Sebastian *et al*, 2012).

Transcriptomic analysis

Microarray services were provided by IRB Functional Genomics Core Facility. Annotation of Affymetrix microarray was performed using Bioconductor R package *mouse4302.db* (Affymetrix Mouse Genome 430 2.0 Array annotation data (chip mouse4302)). Differential expression analysis was carried out using GaGa (Rossell, 2009). Pathway enrichment was assessed through geneset enrichment analysis (GSEA) (Subramanian *et al*, 2005). In these analyses, we used the curated list of genesets included in the Broad Institute Molecular Signature Database (MsigDB-C2) (Subramanian *et al*, 2005). Genes in MsigDB-C2 were translated into *Mus musculus* homolog genes using annotation from the Mouse Genome Informatics (MGI) database (Eppig *et al*, 2015). The complete dataset was deposited to the National Center for Biotechnology Information's Gene Expression Omnibus Database (Barrett & Edgar, 2006) and is accessible through GEO Series accession number GSE71501.

Mitochondrial DNA copy number

Total DNA from tissues or cell cultures was extracted with the DNeasy Blood and Tissue Kit (Quiagen) following the manufacturer's instructions. Mitochondrial DNA was quantified by real-time PCR. Total DNA was used as a template.

Statistical analysis

Data were analyzed by using an appropriate normality test to assess whether the data fit a Gaussian distribution. An *F*-test of equality of variances was performed to demonstrate that the variance between groups was not different. Statistical significance was determined using the Student's *t*-test or analysis of variance (ANOVA) with an appropriate *post hoc* test. Data are presented as mean ± SEM. Significance was established at $P < 0.05$.

Expanded View for this article is available online.

Acknowledgements

We thank the Biostatistics/Bioinformatics Unit, the Functional Genomics Facility and the Histopathology facility from IRB Barcelona, the Unit of Electron Cryo-Microscopy (Scientific and Technological Centers, Universitat de Barcelona), and Jorge Manuel Seco for technological assistance. D. Sala was the recipient of a FPI fellowship from the "Ministerio de Educación y Cultura", Spain. This study was supported by research grants from the MINECO (SAF2013-40987R), Grant 2014SGR48 from the "Generalitat de Catalunya", CIBERDEM ("Instituto de Salud Carlos III"), INTERREG IV-B-SUDOE-FEDER (DIOMED, SOE1/P1/E178), ISCIII (Grant PI13/02512), and FEDER, "María de Maeztu" Programme for Units of Excellence in R&D MDM-2014-0370, AFM, Fundació Marató TV3, and CIBERNED. A.Z. is a recipient of an ICREA "Academia" (Generalitat de Catalunya). IRB Barcelona is the recipient of a Severo Ochoa Award of Excellence from MINECO (Government of Spain).

Author contributions

DSe conceived and performed experiments and wrote the manuscript; ES, JS, AI, DSa, JPM, MS-F, and NP performed experiments; VR-B and ALS performed measurements of muscle force *ex vivo*; EP and AB-L performed transcriptomic analysis; MIH-A, MP, and ALS analyzed the experimental data; AZ directed the research, revised the experimental data, and wrote the manuscript.

Conflict of interest

The authors declare that they have no conflict of interest.

© 2016 The Authors

References

Artal-Sanz M, Tavernarakis N (2009) Prohibitin couples diapause signalling to mitochondrial metabolism during ageing in *C. elegans*. *Nature* 461: 793 – 797

Bach D, Pich S, Soriano FX, Vega N, Baumgartner B, Oriola J, Daugaard JR, Lloberas J, Camps M, Zierath JR, Rabasa-Lhoret R, Wallberg-Henriksson H, Laville M, Palacin M, Vidal H, Rivera F, Brand M, Zorzano A (2003) Mitofusin-2 determines mitochondrial network architecture and mitochondrial metabolism. A novel regulatory mechanism altered in obesity. *J Biol Chem* 278: 17190 – 17197

Barrett T, Edgar R (2006) Gene expression omnibus: microarray data storage, submission, retrieval, and analysis. *Methods Enzymol* 411: 352 – 369

Bellot G, Garcia-Medina R, Gounon P, Chiche J, Roux D, Pouyssegur J, Mazure NM (2009) Hypoxia-induced autophagy is mediated through hypoxia-inducible factor induction of BNIP3 and BNIP3L via their BH3 domains. *Mol Cell Biol* 29: 2570 – 2581

Bernhardt D, Muller M, Reichert AS, Osiewacz HD (2015) Simultaneous impairment of mitochondrial fission and fusion reduces mitophagy and shortens replicative lifespan. *Sci Rep* 5: 7885

Bratic A, Larsson NG (2013) The role of mitochondria in aging. *J Clin Investig* 123: 951 – 957

Brooks SV, Faulkner JA (1988) Contractile properties of skeletal muscles from young, adult and aged mice. *J Physiol* 404: 71 – 82

de Cabo R, Carmona-Gutierrez D, Bernier M, Hall MN, Madeo F (2014) The search for antiaging interventions: from elixirs to fasting regimens. *Cell* 157: 1515 – 1526

Campbell MJ, McComas AJ, Petito F (1973) Physiological changes in ageing muscles. *J Neurol Neurosurg Psychiatry* 36: 174 – 182

Canto C, Pich S, Paz JC, Sanches R, Martinez V, Orpinell M, Palacin M, Zorzano A, Guma A (2007) Neuregulins increase mitochondrial oxidative capacity and insulin sensitivity in skeletal muscle cells. *Diabetes* 56: 2185 – 2193

Carnio S, LoVerso F, Baraibar MA, Longa E, Khan MM, Maffei M, Reischl M, Canepari M, Loefler S, Kern H, Blaauw B, Friguet B, Bottinelli R, Rudolf R, Sandri M (2014) Autophagy impairment in muscle induces neuromuscular junction degeneration and precocious aging. *Cell Rep* 8: 1509 – 1521

Cesari M, Landi F, Vellas B, Bernabei R, Marzetti E (2014) Sarcopenia and physical frailty: two sides of the same coin. *Front Aging Neurosci* 6: 192

Chau NM, Rogers P, Aherne W, Carroll V, Collins I, McDonald E, Workman P, Ashcroft M (2005) Identification of novel small molecule inhibitors of hypoxia-inducible factor-1 that differentially block hypoxia-inducible factor-1 activity and hypoxia-inducible factor-1alpha induction in response to hypoxic stress and growth factors. *Cancer Res* 65: 4918 – 4928

Chen H, McCaffery JM, Chan DC (2007) Mitochondrial fusion protects against neurodegeneration in the cerebellum. *Cell* 130: 548 – 562

Chen KH, Guo X, Ma D, Guo Y, Li Q, Yang D, Li P, Qiu X, Wen S, Xiao RP, Tang J (2004) Dysregulation of HSG triggers vascular proliferative disorders. *Nat Cell Biol* 6: 872 – 883

Chen Y, Dorn GW 2nd (2013) PINK1-phosphorylated mitofusin 2 is a Parkin receptor for culling damaged mitochondria. *Science* 340: 471 – 475

Crane JD, Devries MC, Safdar A, Hamadeh MJ, Tarnopolsky MA (2010) The effect of aging on human skeletal muscle mitochondrial and intramyocellular lipid ultrastructure. *J Gerontol A, Biol Sci Med Sci* 65: 119 – 128

Dela F, Kjaer M (2006) Resistance training, insulin sensitivity and muscle function in the elderly. *Essays Biochem* 42: 75 – 88

Ding Y, Gao H, Zhao L, Wang X, Zheng M (2015) Mitofusin 2-deficiency suppresses cell proliferation through disturbance of autophagy. *PLoS One* 10: e0121328

Eppig JT, Blake JA, Bult CJ, Kadin JA, Richardson JE (2015) The Mouse Genome Database (MGD): facilitating mouse as a model for human biology and disease. *Nucleic Acids Res* 43: D726 – D736

Fitts RH, Troup JP, Witzmann FA, Holloszy JO (1984) The effect of ageing and exercise on skeletal muscle function. *Mech Ageing Dev* 27: 161 – 172

Gomes AP, Price NL, Ling AJ, Moslehi JJ, Montgomery MK, Rajman L, White JP, Teodoro JS, Wrann CD, Hubbard BP, Mercken EM, Palmeira CM, de Cabo R, Rolo AP, Turner N, Bell EL, Sinclair DA (2013) Declining NAD(+) induces a pseudohypoxic state disrupting nuclear-mitochondrial communication during aging. *Cell* 155: 1624 – 1638

Goodman CA, Mabrey DM, Frey JW, Miu MH, Schmidt EK, Pierre P, Hornberger TA (2011) Novel insights into the regulation of skeletal muscle protein synthesis as revealed by a new nonradioactive in vivo technique. *FASEB J* 25: 1028 – 1039

Hailey DW, Rambold AS, Satpute-Krishnan P, Mitra K, Sougrat R, Kim PK, Lippincott-Schwartz J (2010) Mitochondria supply membranes for autophagosome biogenesis during starvation. *Cell* 141: 656 – 667

Hamalainen N, Pette D (1993) The histochemical profiles of fast fiber types IIB, IID, and IIA in skeletal muscles of mouse, rat, and rabbit. *J Histochem Cytochem* 41: 733 – 743

Heidt AB, Black BL (2005) Transgenic mice that express Cre recombinase under control of a skeletal muscle-specific promoter from mef2c. *Genesis* 42: 28 – 32

Kroemer G (2015) Autophagy: a druggable process that is deregulated in aging and human disease. *J Clin Investig* 125: 1 – 4

Lanza IR, Nair KS (2010) Mitochondrial function as a determinant of life span. *Pflugers Archiv* 459: 277 – 289

Leduc-Gaudet JP, Picard M, Pelletier FS, Sgarioto N, Auger MJ, Vallee J, Robitaille R, St-Pierre DH, Gouspillou G (2015) Mitochondrial morphology is altered in atrophied skeletal muscle of aged mice. *Oncotarget* 6: 17923 – 17937

Liesa M, Palacin M, Zorzano A (2009) Mitochondrial dynamics in mammalian health and disease. *Physiol Rev* 89: 799 – 845

Liesa M, Shirihai OS (2013) Mitochondrial dynamics in the regulation of nutrient utilization and energy expenditure. *Cell Metab* 17: 491 – 506

Marzetti E, Calvani R, Cesari M, Buford TW, Lorenzi M, Behnke BJ, Leeuwenburgh C (2013) Mitochondrial dysfunction and sarcopenia of aging: from signaling pathways to clinical trials. *Int J Biochem Cell Biol* 45: 2288 – 2301

Masiero E, Agatea L, Mammucari C, Blaauw B, Loro E, Komatsu M, Metzger D, Reggiani C, Schiaffino S, Sandri M (2009) Autophagy is required to maintain muscle mass. *Cell Metab* 10: 507 – 515

Masiero E, Sandri M (2010) Autophagy inhibition induces atrophy and myopathy in adult skeletal muscles. *Autophagy* 6: 307 – 309

Munoz JP, Ivanova S, Sanchez-Wandelmer J, Martinez-Cristobal P, Noguera E, Sancho A, Diaz-Ramos A, Hernandez-Alvarez MI, Sebastian D, Mauvezin C, Palacin M, Zorzano A (2013) Mfn2 modulates the UPR and mitochondrial function via repression of PERK. *EMBO J* 32: 2348 – 2361

Ngoh GA, Papanicolaou KN, Walsh K (2012) Loss of mitofusin 2 promotes endoplasmic reticulum stress. *J Biol Chem* 287: 20321 – 20332

Niccoli T, Partridge L (2012) Ageing as a risk factor for disease. *Current Biol* 22: R741 – R752

Ojaimi J, Masters CL, Opeskin K, McKelvie P, Byrne E (1999) Mitochondrial respiratory chain activity in the human brain as a function of age. *Mech Ageing Dev* 111: 39 – 47

 © 2016 The Authors

Palikaras K, Lionaki E, Tavernarakis N (2015) Coordination of mitophagy and mitochondrial biogenesis during ageing in *C. elegans*. *Nature* 521: 525 – 528

Patten DA, Lafleur VN, Robitaille GA, Chan DA, Giaccia AJ, Richard DE (2010) Hypoxia-inducible factor-1 activation in nonhypoxic conditions: the essential role of mitochondrial-derived reactive oxygen species. *Mol Biol Cell* 21: 3247 – 3257

Pessina P, Cabrera D, Morales MG, Riquelme CA, Gutierrez J, Serrano AL, Brandan E, Munoz-Canoves P (2014) Novel and optimized strategies for inducing fibrosis in vivo: focus on Duchenne Muscular Dystrophy. *Skelet Muscle* 4: 7

Preston CC, Oberlin AS, Holmuhamedov EL, Gupta A, Sagar S, Syed RH, Siddiqui SA, Raghavakaimal S, Terzic A, Jahangir A (2008) Aging-induced alterations in gene transcripts and functional activity of mitochondrial oxidative phosphorylation complexes in the heart. *Mech Ageing Dev* 129: 304 – 312

Rolfe DF, Brown GC (1997) Cellular energy utilization and molecular origin of standard metabolic rate in mammals. *Physiol Rev* 77: 731 – 758

Romanello V, Guadagnin E, Gomes L, Roder I, Sandri C, Petersen Y, Milan G, Masiero E, Del Piccolo P, Foretz M, Scorrano L, Rudolf R, Sandri M (2010) Mitochondrial fission and remodelling contributes to muscle atrophy. *EMBO J* 29: 1774 – 1785

Ross JM (2011) Visualization of mitochondrial respiratory function using cytochrome c oxidase/succinate dehydrogenase (COX/SDH) double-labeling histochemistry. *J Vis Exp* 57: e3266

Rossell D (2009) GaGa: a parsimonious and flexible model for differential expression analysis. *Ann Appl Stat* 3: 1035 – 1051

Sala D, Ivanova S, Plana N, Ribas V, Duran J, Bach D, Turkseven S, Laville M, Vidal H, Karczewska-Kupczewska M, Kowalska I, Straczkowski M, Testar X, Palacin M, Sandri M, Serrano AL, Zorzano A (2014) Autophagy-regulating TP53INP2 mediates muscle wasting and is repressed in diabetes. *J Clin Investig* 124: 1914 – 1927

Salminen A, Kaarniranta K (2009) Regulation of the aging process by autophagy. *Trends Mol Med* 15: 217 – 224

Scheckhuber CQ, Erjavec N, Tinazli A, Hamann A, Nystrom T, Osiewacz HD (2007) Reducing mitochondrial fission results in increased life span and fitness of two fungal ageing models. *Nat Cell Biol* 9: 99 – 105

Sebastian D, Hernandez-Alvarez MI, Segales J, Sorianello E, Munoz JP, Sala D, Waget A, Liesa M, Paz JC, Gopalacharyulu P, Oresic M, Pich S, Burcelin R, Palacin M, Zorzano A (2012) Mitofusin 2 (Mfn2) links mitochondrial and endoplasmic reticulum function with insulin signaling and is essential for normal glucose homeostasis. *Proc Natl Acad Sci USA* 109: 5523 – 5528

Segales J, Paz JC, Hernandez-Alvarez MI, Sala D, Munoz JP, Noguera E, Pich S, Palacin M, Enriquez JA, Zorzano A (2013) A form of mitofusin 2 (Mfn2) lacking the transmembrane domains and the COOH-terminal end stimulates metabolism in muscle and liver cells. *Am J Physiol Endocrinol Metab* 305: E1208 – E1221

Serrano AL, Murgia M, Pallafacchina G, Calabria E, Coniglio P, Lomo T, Schiaffino S (2001) Calcineurin controls nerve activity-dependent specification of slow skeletal muscle fibers but not muscle growth. *Proc Natl Acad Sci USA* 98: 13108 – 13113

Shigenaga MK, Hagen TM, Ames BN (1994) Oxidative damage and mitochondrial decay in aging. *Proc Natl Acad Sci USA* 91: 10771 – 10778

Short KR, Bigelow ML, Kahl J, Singh R, Coenen-Schimke J, Raghavakaimal S, Nair KS (2005) Decline in skeletal muscle mitochondrial function with aging in humans. *Proc Natl Acad Sci USA* 102: 5618 – 5623

Song M, Mihara K, Chen Y, Scorrano L, Dorn GW 2nd (2015) Mitochondrial fission and fusion factors reciprocally orchestrate mitophagic culling in mouse hearts and cultured fibroblasts. *Cell Metab* 21: 273 – 285

Strucksberg KH, Tangavelou K, Schroder R, Clemen CS (2010) Proteasomal activity in skeletal muscle: a matter of assay design, muscle type, and age. *Anal Biochem* 399: 225 – 229

Subramanian A, Tamayo P, Mootha VK, Mukherjee S, Ebert BL, Gillette MA, Paulovich A, Pomeroy SL, Golub TR, Lander ES, Mesirov JP (2005) Gene set enrichment analysis: a knowledge-based approach for interpreting genome-wide expression profiles. *Proc Natl Acad Sci USA* 102: 15545 – 15550

Twig G, Elorza A, Molina AJ, Mohamed H, Wikstrom JD, Walzer G, Stiles L, Haigh SE, Katz S, Las G, Alroy J, Wu M, Py BF, Yuan J, Deeney JT, Corkey BE, Shirihai OS (2008) Fission and selective fusion govern mitochondrial segregation and elimination by autophagy. *EMBO J* 27: 433 – 446

Williamson DL, Kubica N, Kimball SR, Jefferson LS (2006) Exercise-induced alterations in extracellular signal-regulated kinase 1/2 and mammalian target of rapamycin (mTOR) signalling to regulatory mechanisms of mRNA translation in mouse muscle. *J Physiol* 573: 497 – 510

Yang CC, Chen D, Lee SS, Walter L (2011) The dynamin-related protein DRP-1 and the insulin signaling pathway cooperate to modulate Caenorhabditis elegans longevity. *Aging Cell* 10: 724 – 728

Yasukawa K, Oshiumi H, Takeda M, Ishihara N, Yanagi Y, Seya T, Kawabata S, Koshiba T (2009) Mitofusin 2 inhibits mitochondrial antiviral signaling. *Sci Signal* 2: ra47

Zhang H, Bosch-Marce M, Shimoda LA, Tan YS, Baek JH, Wesley JB, Gonzalez FJ, Semenza GL (2008) Mitochondrial autophagy is an HIF-1-dependent adaptive metabolic response to hypoxia. *J Biol Chem* 283: 10892 – 10903

Zhao L, Zou X, Feng Z, Luo C, Liu J, Li H, Chang L, Wang H, Li Y, Long J, Gao F (2014) Evidence for association of mitochondrial metabolism alteration with lipid accumulation in aging rats. *Exp Gerontol* 56: 3 – 12

Zhao T, Liang D, Wang P, Liu J, Ma F (2012) Genome-wide analysis and expression profiling of the DREB transcription factor gene family in Malus under abiotic stress. *Mol Genet Genomics* 287: 423 – 436

© 2016 The Authors